Volume 44, Number 4 October, 2020

Technical Soaring

An International Journal

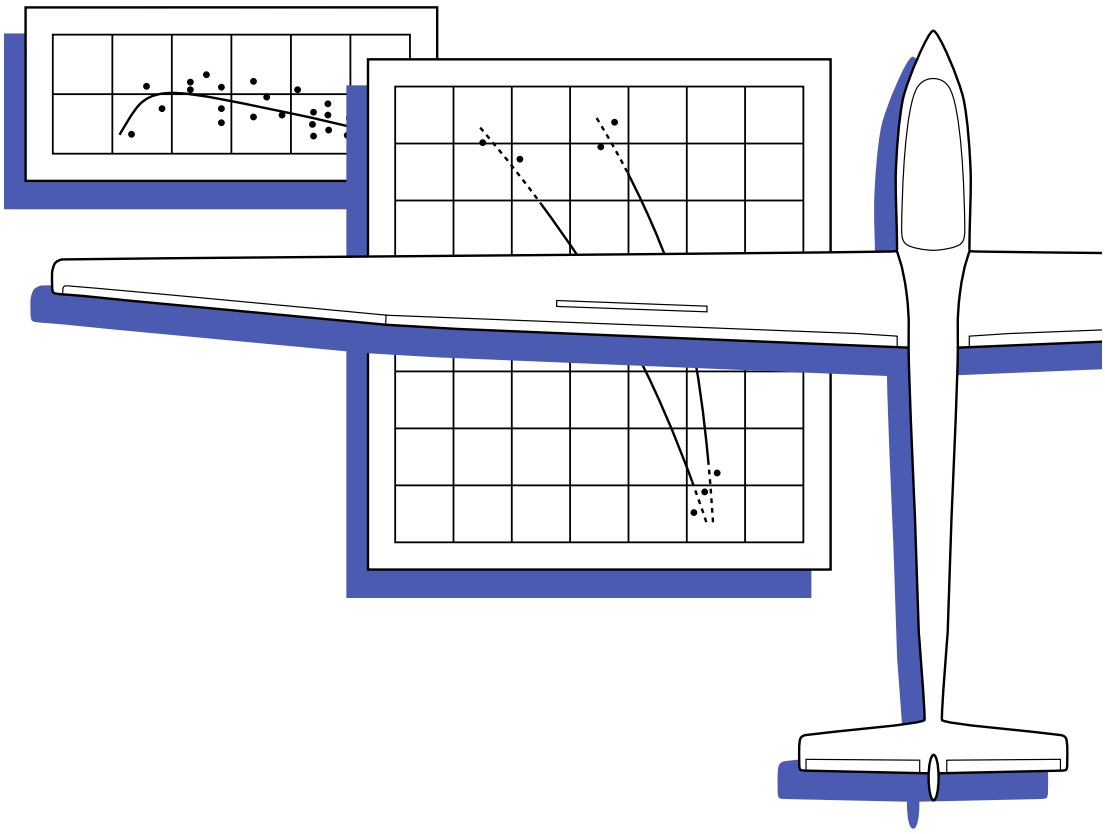

- **Validating mountain-wave predictions**

Organisation Scientifique et Technique Internationale du Vol à Voile (OSTIV)
International Scientific and Technical Organization for Soaring
www.ostiv.org

Technical Soaring

The Scientific, Technical and Operational Journal of
the Organisation Scientifique et Technique Internationale du Vol à Voile
(International Scientific and Technical Organization for Soaring)

Volume 44, Number 4 **October — December 2020**

ISSN 0744-8996

Technical Soaring (*TS*) documents recent advances in the science, technology and operations of motorless aviation.
TS is published quarterly by the Organisation Scientifique et Technique Internationale du Vol à Voile (International Scientific and Technical Organization for Soaring, OSTIV), c/o TU Braunschweig, Institute of Fluid Mechanics, Hermann-Blenk Str. 37, D-38108 Braunschweig, Germany. E-mail: `president@ostiv.org`; URL: `www.ostiv.org`.
Subscription is restricted to OSTIV members but material can be submitted by anyone. Annual dues are €25 for Individual/Local Club Membership; €80 for Scientific/Technical Organization/Library Membership and €250 for Active Members (National Aero Club Members of FAI). Students under 25 years of age may join free of charge.
Submitted research papers will be peer-reviewed. Guidelines for preparation and submission of manuscripts can be found in this issue and on the OSTIV website in the 'editor' section.
TS is online (full-color) at `journals.sfu.ca/ts/`. Back issues, from Vol. 1, No. 1 to the current issue are online. OSTIV members have complete access to *TS* online; non-members may access titles and abstracts. Members should contact the webmaster, `Jannes.Neumann@t-online.de`, for access.

Preparation of Manuscripts for *Technical Soaring*

Technical Soaring (*TS*) documents recent advances in the science, technology and operations of motorless aviation. *TS* welcomes original contributions from all sources.

General Requirements Manuscripts must be unclassified and cleared for public release. The work must not infringe on copyrights, and must not have been published or be under consideration for publication elsewhere. Authors must sign and submit a copyright form at time of submission. The form is available at `www.ostiv.org`.

Language All manuscripts submitted to *TS* must be in English. Submissions requiring extensive editing may be returned to author for proofreading and correction prior to review.

Layout Submit manuscripts in single-column, double spaced layout with all figures and tables at end, one per page.

Electronic submissions are preferred. Most data file formats are acceptable, with PDF preferred. Submit one file containing the complete paper including all figures, tables, and captions. Paper submissions will also be accepted — contact the Editor-in-chief (EIC) for submission details.

Length There is no fixed length limit. At the discretion of the EIC, manuscripts may be returned to the author for reduction in length.

Structure Organize papers as needed in sections, subsections, and subsubsections.

Title A title block is required with author name(s), affiliation(s), location, and contact info (email address preferred).

Abstract All papers require a summary-type abstract consisting of a single, self-contained paragraph. Suggest 100 to 150 words. Acronyms may be introduced in the abstract, but do not cite references, figures, tables, or footnotes.

Nomenclature If the paper uses more than a few symbols, list and define them in a separate table. Otherwise, explain them in the text where first used. Define acronyms in the text following first use.

Introduction An Introduction is required that states the purpose of the work and its significance with respect to prior literature, and allows the paper to be understood without undue reference to other sources.

Conclusions The Conclusions section should review the main points of the paper. Do not simply replicate the abstract. Do not introduce new material or cite references, figures, or tables in the Conclusions section.

Acknowledgments Inclusion of support and/or sponsorship acknowledgments is strongly encouraged.

Citations Cite with bibliographic reference numbers in brackets (e.g. "[7]"). Do not cite Internet URLs unless the website itself is the subject of discussion.

References All references listed in the References section must be cited in the text. List references in order of first citation in the text. Any format is acceptable as long as all citation data are provided. At a minimum, all types of entries require title, year and manner of publication. Provide full names of all authors. Do not list Internet URLs as sources.

Captions All figures and tables require captions. Do not use the caption to explain line styles and symbols — use a legend instead.

Color Color graphics are acceptable. Avoid using color to distinguish data sets in figures — instead, use line styles, symbol shapes and fill patterns.

Footnotes Use footnotes sparingly. Do not footnote to cite literature.

Numbering All figures, tables, footnotes and references must be referenced in the text and are numbered sequentially in order of first reference. Equations are numbered only if they are referenced by number in the text. Number every page.

How to submit Email all electronic material to the EIC at `ts-editor@ostiv.org` and contact the EIC at `arne.seitz@dlr.de` if acknowledgement is not received.

Peer Review Manuscripts will be peer-reviewed before being accepted for publication. Authors may choose between two options: A full peer review with two independent and anonymous reviewers. In this case authors are welcome to suggest names of reviewers. The second option is the *TS* Fast Track Scheme, with the manuscript being reviewed by the EIC or an Associate Editor. With the publication of an article it will be documented in a footnote on the first page of the article which option was chosen by the author. The EIC or the assigned Associate Editor may be contacted by the author at any time for updates on the status of their review.

Charges *Technical Soaring* does not require a publication page-charge.

From the Editor

Publication Date

This issue is the fourth of Volume 44 of *TS*, corresponding to October-December 2020. For the record, the issue was published in November, 2020.

Acknowledgements

We gratefully acknowledge Associate Editor Götz Bramesfeld, who oversaw the review of the Hindman paper in this issue.

Very Respectfully,

Arne Seitz
Editor-in-Chief, *Technical Soaring*
ts-editor@ostiv.org

Validating mountain-wave predictions from the United States High-Resolution, Rapid-Refresh (HRRR) numerical weather prediction (NWP) model

Edward Hindman
ehindman@ccny.cuny.edu
Earth and Atmospheric Sciences Department
The City College of New York, New York, NY, USA

Abstract

The National Oceanic and Atmospheric Administration (NOAA) has developed the HRRR NWP model and made the predictions available, free-of-charge, at *rapidrefresh.noaa.gov/hrrr/*. The model is sufficiently high-resolution to predict mountain waves. The waves appear in the 'max updraft' maps as linear and quasi-linear regions. In this study, glider flight recorder data from eastern US wave flights are compared with these regions. It is shown the regions, indeed, contained mountain waves. A number of the flights achieved the 5-km altitude-gain for the Fédération Aéronautique Internationale (FAI) Diamond Badge. The predicted updraft speeds, on average, were consistent with the updraft speeds calculated from the flight recorder data.

Introduction

Climbs to achieve the altitude requirement for FAI soaring badges are often made in mountain waves. Thus, forecasts of these conditions are essential. The first report in the OSTIV literature about detecting and forecasting their occurrence is described in [1]. Since that report, there has been tremendous progress. Currently real-time images of satellite-detected mountain- wave clouds and corresponding forecasts are at one's fingertips through the Internet. Probably the most up-to-date system is described in [2] and a remarkable wave flight using the system is described in [3].

In the winter of 2015-16, I was asked by northeast US wave pilot Timothy Chow to help interpret the freely-available HRRR NWP model 'max updraft' forecasts. The forecasts depicted linear updraft regions resembling waves in mountainous regions. Thus, I compared his flight recorder data, and that of other northeast US wave pilots, with the corresponding HRRR model forecasts. As reported here, I found the regions, indeed, contained mountain waves and the predicted updraft speeds were, on average, consistent with measured speeds. This paper completes the extended abstract from the 2018 Congress [4] and incorporates suggestions from the attendees.

Methods

The forecasts were validated using the following procedure. The locations of the high-points of wave flights and the maximum rate-of-climb to those points were determined from glider flight records (*.igc files). Then, those locations were identified on the 'max updraft' prediction charts (*.png files) and the magnitude of the updrafts were recorded. The measured and predicted updraft values, then, were compared.

Eight eastern US wave flights were investigated. The procedure will be detailed for the first flight.

On 20160204 (Flight 1), Timothy Chow made a wave flight in the Green Mountains of Vermont. The high-point of the flight was determined from his *.igc file. The file was displayed in SeeYou. The barogram trace was animated to the high-point and the time, altitude and latitude/longitude at that point were recorded.

The high-point was located on the corresponding HRRR model 'max updraft' *.png image using the image analysis software ArcSoft:

1. The image was expanded to extract x, y values of unique ground-points. Latitude and longitude values for the points were determined using the *skyvector.com* aeronautical chart.

2. An x-y grid with superimposed latitude and longitude values of the ground-points was constructed. The pixel corresponding to the latitude and longitude of the high point was determined by interpolation and recorded.

3. The Red Green Blue (RGB) values of the pixel were compared to the RGB values of the updraft speed scale on the image. The closest match was defined as the predicted updraft speed; for the Chow flight the speed was 0 - 0.5 m/s. The predicted updraft was recorded (see Table 1).

This article was peer reviewed by two independent, anonymous reviewers.
Presented at the XXXIV OSTIV Congress, Letiště Hosín, Czech Republic, 28 July – 3 August, 2018

Flight	Date	Time	Altitude	+ alt	t	- alt	t	del t	Climb rate	Sink-rate	Measured	Predicted
		UTC	m AMSL	m AMSL	hhmmss	m AMSL	hhmmss	s	m/s	m/s	m/s	m/s
1	20160204	165844	2520	3020	170204	2020	165548	376	2.7	0.9	3.6	0.5
2	20160206	185700	4274	4522	185940	4094	185340	360	1.2	0.7	1.9	0.75
3	20161010	163629	4250	4750	164054	3750	163150	536	1.9	0.6	2.4	2.3
4	20161014	193614	3500	3750	194102	3250	193118	584	0.9	0.5	1.3	0.75
5	20171117	180901	3000	3250	181259	2750	180450	469	1.1	0.6	1.7	1.8
6	20171126	153712	3500	3750	154010	3250	153438	332	1.5	0.6	2.1	3.8
7	20180127	154536	4500	4750	154848	4250	154243	366	1.4	0.8	2.1	2.25
8	20180205	143000	3250	3500	143158	3000	142812	226	2.2	0.8	3.0	3.8
	AVERAGE								1.6		2.3	2.0

Table 1: Measured and predicted updraft speeds.

4. The pixel in the *.png image that corresponded to the high point was colored red.

5. The pixel in the *.png image that corresponded to the summit to the west of Chow's high-point was colored green. Similarly, the pixels corresponding to locations of mountain summits where the other wave flights reported here were made were colored green: Mt. Washington in the White Mountains of NH, Sugarbush Peak in the Green Mountains of VT and Slide Mountain in the Catskill Mountains of NY.

The high-point for Chow's flight, the predicted updraft regions and the mountain summits are illustrated in Fig. 1 (top row left).

The HRRR model atmospheric profiles for the location, date and time of the high-points were retrieved from the National Oceanic and Atmospheric Administration (NOAA). The atmospheric conditions were determined from the profiles. The profile for Chow's flight is given in Fig. 1 (top row center). This profile (+1h) is the closest in the archive to the initialization profile (0h). The 0h profile was not available in the archive.

The satellite visible-image nearest in time to Chow's high point is given in Fig. 1 (top row right).

The maximum climb rate achieved in the region of the wave at which the high-point was reached was determined from the *.igc file for Flight 1 as illustrated in Table 1. The heading in Table 1 is defined from left-to-right as follows: 'Time' is the time the maximum rate-of-climb was achieved (steepest barogram slope) in the region of the wave that led to the high-point, 'Altitude' is the altitude bisecting the steepest slope, '+ alt' is the altitude at the top of the bisected slope, 't' is the time at the + alt, '– alt' is the altitude at the bottom of the bisected slope, 't' is the time at the - alt, 'del t' is the interval to climb from below to above the altitude with steepest slope, 'Climb rate' is equal to the difference between +alt and -alt divided by del t, 'Sink rate' is from the glider's polar, 'Measured' is the climb rate plus the sink speed, 'Predicted' is the HRRR model updraft prediction. The 'Altitude' values are less than the maximum altitudes achieved because the 'Climb rate' values were determined before the high-point was achieved.

The climb rate was adjusted to account for the headwind as follows. From the PIK-20D polar (Chow's aircraft), the minimum sink rate is 0.58 m/s at 40 knots (73 km/h). Using a indicated airspeed (IAS) - to - true airspeed (TAS) calculator (*indoavis.co.id/main/tas.html*) and atmospheric conditions from Fig. 1 (center), the IAS was 68 knots (124 km/h) for Chow to remain stationary in the wave and the TAS was 69 knots (126 km/h). The sink rate of the ship in still-air at 126 kph from the polar is 0.9 m/s. So, the measured maximum updraft was 2.7 + 0.9 m/s = 3.6 m/s. The value was recorded (see Table 1).

Seven additional flights were similarly analyzed: Timothy Chow's 20160206 flight (Flight 2) in the Sugarbush wave in Vermont, Paul Villinski's 20161010 flight (Flight 3) in the Mt. Washington wave of New Hampshire and Roy Bourgeois's

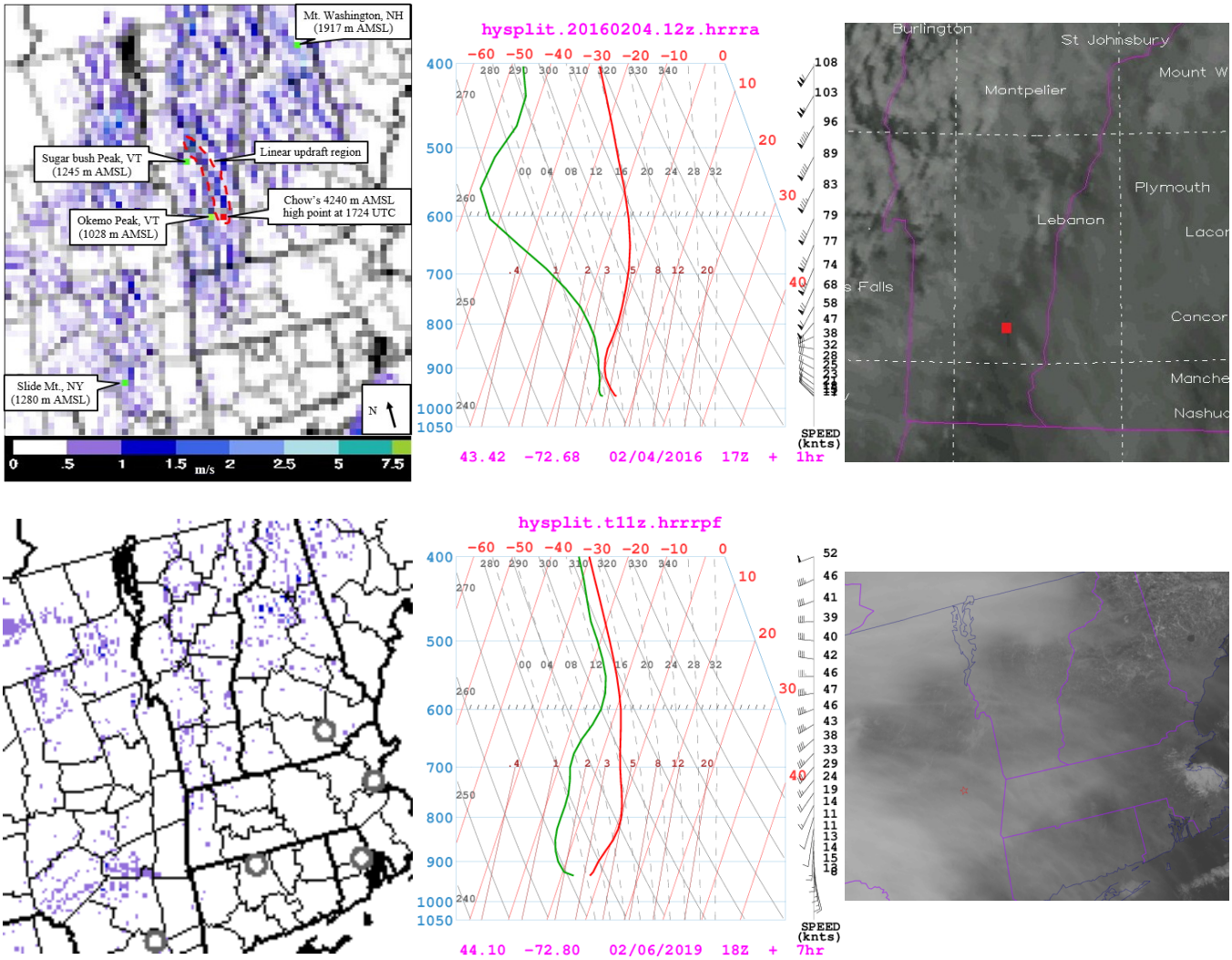

Fig. 1: Top row: Left, 20160204, HRRR model 7h forecast valid at 1700UTC (1200LT) for the maximum updraft speed (m/s) surface to 100 mb over the previous hour. Labeled is the high-point of Tim Chow's flight (red pixel), the linear updraft region (dashed red line) and the location of the mountains (green pixels) that produced the wave. Center, the atmospheric profile for the location, date and time of the highpoint. Right, visible image at 1745UTC from GOES-E illustrating the approximate location of the high-point (red square).
Bottom row: Left-to-right, 20190206, HRRR model 9h forecast valid at 1800UTC, corresponding sounding near Sugarbush Pk. and GOES-E image.

20161014 flight (Flight 4) in the Mt. Washington wave and Daniel Sazhin's 20171117, 20171126, 20180127 and 20180205 flights (Flights 5 – 8) in the Slide Mountain wave of the Catskill Mountains of New York. The results are displayed in Fig. 2 through Fig. 8 and in Table 1.

Results

It can be seen from Fig. 1 (left) that Chow's high-point was 4240 m AMSL (altitude gain 2597 m, Silver Badge climb) in a linear updraft region just downwind of Okemo Peak. The maximum predicted updraft speed for that location was 0 - 0.5 m/s and the maximum climb rate was 3.6 m/s passing through 2520 m AMSL (Table 1). This altitude corresponds to approximately the 750 mb level where, from Fig. 1 (center), the winds were from 205 degrees-true at 68 knots. The GOES-E image, Fig. 1 (right), shows wave clouds in the vicinity of the high-point validating the moist layer in the profile. Additionally, it can be seen wave clouds are oriented consistent with the predicted linear updraft region.

Shown in the bottom row of Fig. 1 is a forecast for the same region in light-wind conditions. It can be seen no linear updraft regions were predicted and no waves are visible in the high, thin cirrus. Additionally, the atmosphere is too stable to support convection hence no convective clouds are visible through the thin

cirrus.

It can be seen from Fig. 2 (left), that Chow's high-point was 4610 m AMSL in a linear updraft region just downwind of the NW-SE oriented ridge of that contains Sugarbush Peak (altitude gain 2700 m, Silver Badge climb). The maximum predicted updraft for that location corresponded to 0.5 - 1 m/s (∼0.75 m/s) and the maximum climb rate was 1.9 m/s passing through 4247 m AMSL (Table 1). This altitude corresponds to approximately the 600 mb level where, from Fig. 2 (center), the winds were from 235 degrees-true at 60 knots. The GOES-E image, Fig. 2 (right), shows wave clouds oriented in a direction similar to the orientation of the predicted linear updraft region.

It can be seen from Fig. 3 (left), that Villinski's high-point was 6412 m AMSL in a quasi-linear updraft region just downwind of Mt. Washington (altitude gain 4818 m, Gold Badge climb). The maximum predicted updraft speed for that location was 2 – 2.5 m/s (∼2.3 m/s) and the maximum climb rate was 2.4 m/s passing through 4250 m AMSL (Table 1). This altitude corresponds to approximately the 600 mb level where, from Fig. 3 (center), the winds were from 360 degrees-true at 45 knots. The GOES-E image, Fig. 3 (right), shows clouds induced by the White Mountains; a surface air parcel forced to lift to the 800mb height of the mountains would produce a 'cap' cloud. Above this cloud, the atmosphere was too dry for the wave to produce lenticular clouds, hence none are visible in the GOES-E image.

It can be seen from Fig. 4 (left) that Bourgeois's high-point was 4505 m AMSL in a quasi-linear updraft region just downwind of the SW-NE oriented ridge of Mt. Washington (altitude gain, 3300 m, Gold Badge climb). The maximum predicted updraft for that location corresponded to ∼0.75 m/s and the maximum climb rate was 1.3 m/s passing through 3500 m AMSL (Table 1). The 3500 m altitude corresponds to approximately the 660 mb level where, from Fig. 4 (center), the winds were from 320 degrees-true at 25 knots. The GOES-E image, Fig. 4 (right), is dark due to the low sun angle and a lack of clouds. The absence of clouds is consistent with the dry atmospheric profile.

It can be seen from Fig. 5 (left), that Sazhin's high-point was 5435 m AMSL in a linear updraft region just downwind of the SW-NE oriented west-ridge of Slide Mountain (altitude gain 5095 m, Diamond Badge climb). The maximum predicted updraft for that location corresponded to ∼1.8 m/s and the maximum climb rate was 1.1 m/s passing through 3000 m AMSL (Table 1). The 3000 m altitude corresponds to approximately the 700 mb level where, from Fig. 5 (center), the winds were from 350 degrees-true at 40 knots. The GOES-E visible image, Fig. 5 (right), shows a faint, low cloud line below and downwind of Sazhin's high point. The line was faint due the low sun-angle. The line was low because it formed, most likely, in the wake of Slide Mountain; similar cloud lines appear in Fig. 6 (right) and Fig. 8 (right). Cloud lines orthogonal to waves above are common in this region [5]. Reference [3] details Sazhin's extraordinary flight.

It can be seen from Fig. 6 (left), that Sazhin's high-point was 5447 m AMSL in a linear updraft region just downwind of the SW-NE oriented west-ridge of Slide Mountain (the altitude gain was 5038 m, Diamond Badge climb). The maximum predicted updraft at that location corresponded to 3.8 m/s and the maximum climb rate was 2.1 m/s passing through 3500 m AMSL (Table 1). The 3500 m altitude corresponds to approximately the

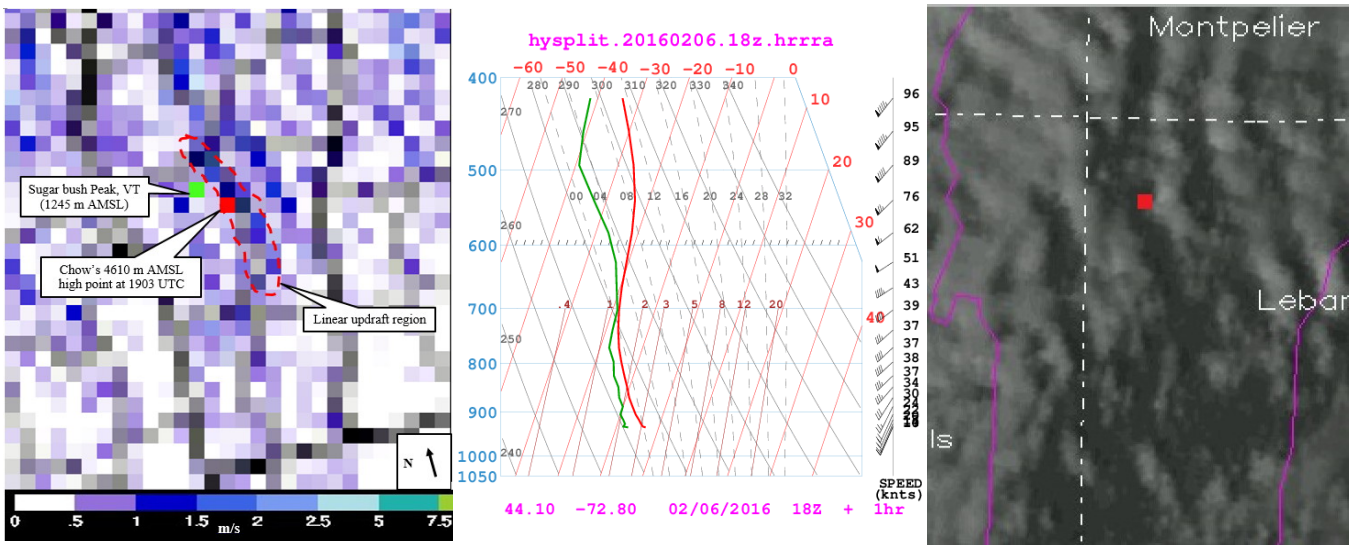

Fig. 2: Left, 20160206, HRRR model 1h forecast valid at 1800UTC (1300LT) for the maximum updraft speed (m/s) surface to 100 mb over the previous hour. Labeled is the high-point of Tim Chow's flight (red pixel), the linear updraft region (dashed red line) and the location of the mountain summit (green pixel) on the ridge that triggered the significant wave. Center, the atmospheric profile for the location, date and time of the high-point. Right, visible image at 1900UTC from GOES-E illustrating the approximate location of the highpoint (red square).

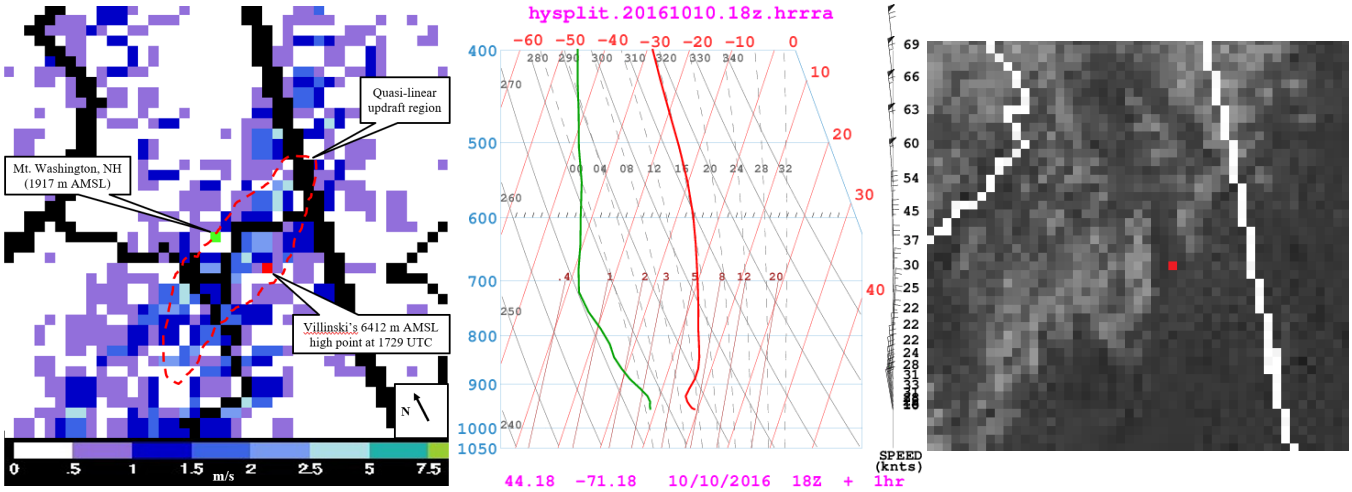

Fig. 3: Left, 20161010, HRRR model 6h forecast valid at 1800UTC (1300LT) for the maximum updraft speed (m/s) surface to 100 mb over the previous hour. Labeled is the high-point of Paul Villinski's flight (red pixel), the quasi-linear updraft region (dashed red line) and the location of the mountain summit (green pixel) on the ridge that triggered the wave. Center, the atmospheric profile for the location, date and time of the high-point. Right, visible image at 1715UTC from GOES-E illustrating the approximate location of the high-point (red square).

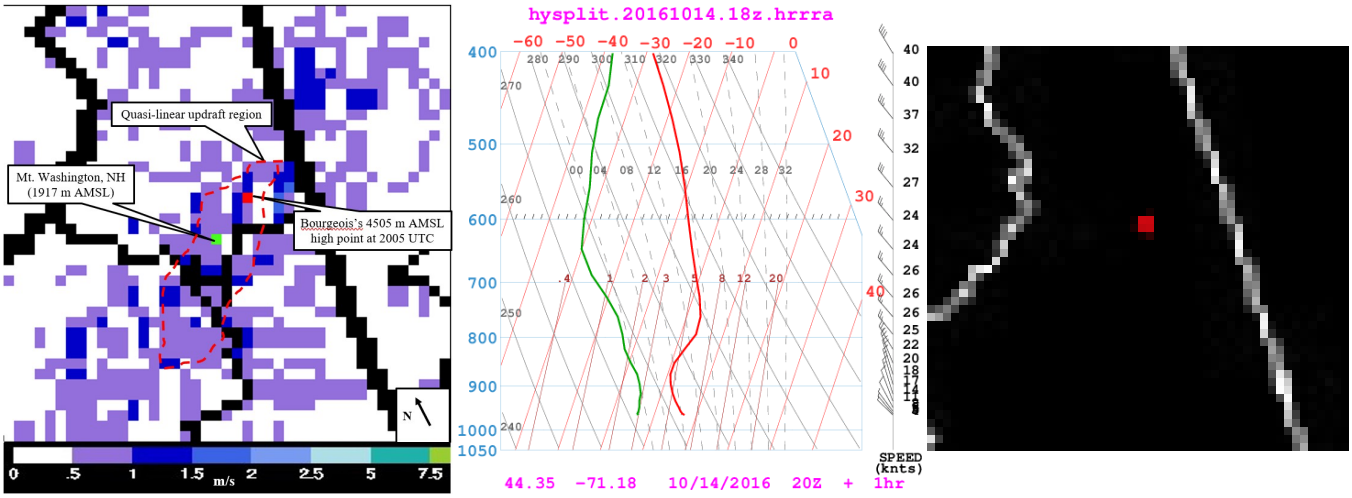

Fig. 4: Left, 20161014, HRRR model 13h forecast valid at 2000UTC (1500LT) for the maximum updraft speed (m/s) surface to 100 mb over the previous hour. Labeled is the high-point of Roy Bourgeois's flight (red pixel), the quasi-linear updraft region (dashed red line) and the location of the mountain summit (green pixel) on the ridge that triggered the wave. Center, the atmospheric profile for the location, date and time of the high-point. Right, visible image at 2000UTC from GOES-E illustrating the approximate location of the high-point (red square).

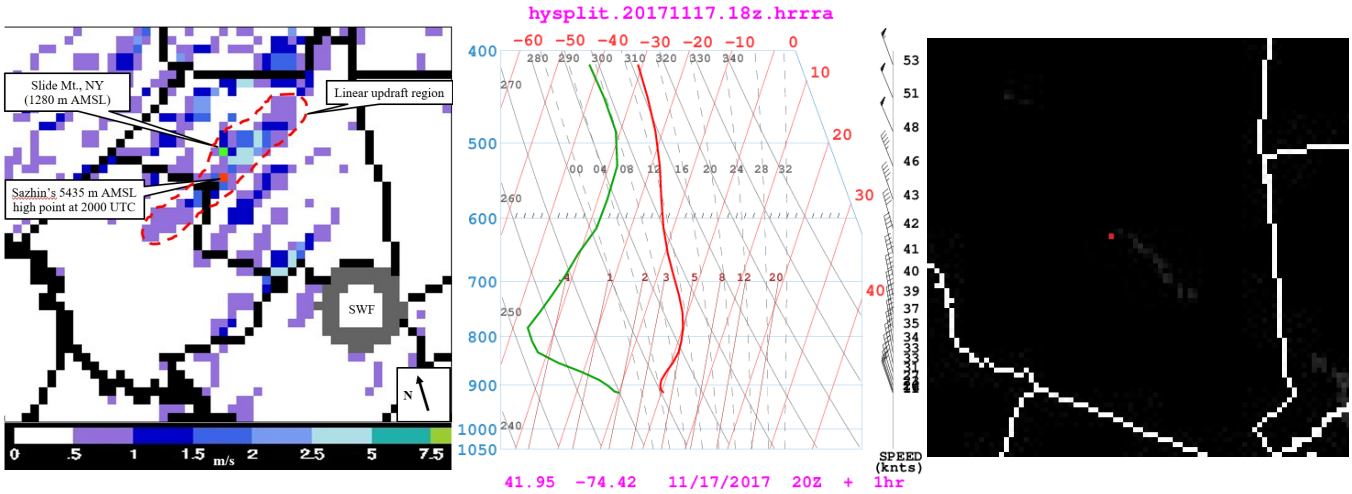

Fig. 5: Left, 20171117, HRRR model 10h forecast valid at 2000UTC (1500LT) for the maximum updraft speed (m/s) surface to 100 mb over the previous hour. Labeled is the high-point of Daniel Sazhin's flight (red pixel), the linear updraft region (dashed red line), the location of the mountain summit (green pixel) on the ridge that triggered the wave and Steward Field (SWF). Center, the atmospheric profile for the location, date and time of the high-point. Right, visible image at 1945UTC from GOES-E illustrating the approximate location of the high-point (red square).

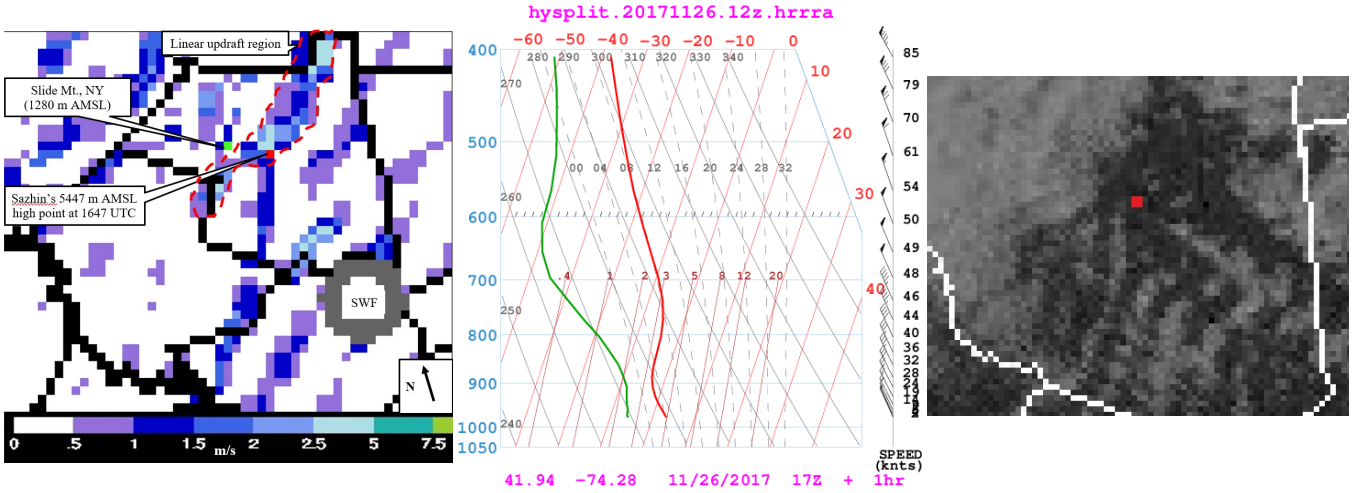

Fig. 6: Left, 20171126, HRRR model 10h forecast valid at 1700UTC (1200LT) for the maximum updraft speed (m/s) surface to 100 mb over the previous hour. Labeled is the high-point of Daniel Sazhin's flight (red pixel), the linear updraft region (dashed red line), the location of the mountain summit (green pixel) on the ridge that triggered the wave and Steward Field (SWF). Center, the atmospheric profile for the location, date and time of the high-point. Right, visible image at 1645UTC from GOES-E illustrating the approximate location of the high-point (red square).

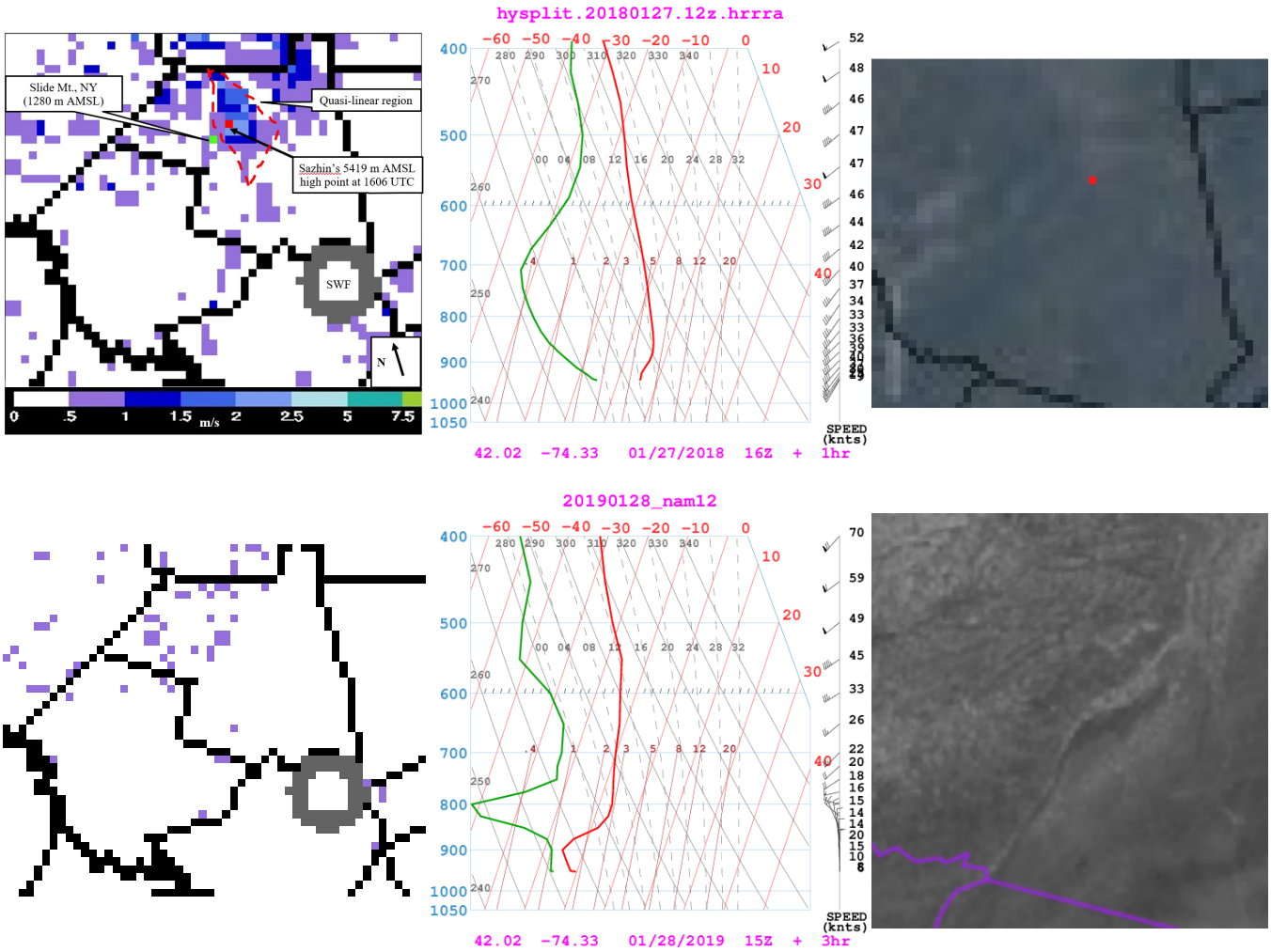

Fig. 7: Top row: Left, 20180127, HRRR model 6h forecast valid at 1600UTC (1100LT) for the maximum updraft speed (m/s) surface to 100 mb over the previous hour. Labeled is the high-point of Daniel Sazhin's flight (red pixel), the quasi-linear updraft region (dashed red line), the location of the mountain summit (green pixel) on the ridge that triggered the wave and Steward Field (SWF). Center, the atmospheric profile for the location, date and time of the high-point. Right, visible image at 1603UTC from GOES-E illustrating the approximate location of the high-point (red square).
Bottom row: Left-to-right, 20190128 HRRR model 4h forecast valid at 1600UTC, corresponding sounding near Slide Mt. and GOES-E image.

660 mb level where, from Fig. 6 (center), the winds were from 335 degrees-true at 45 knots. The GOES-E visible image, Fig. 6 (right), reveals wave clouds consistent with the orientation of the predicted linear- updraft regions. Additionally, a cloud line appears in the wake of Slide mountain, similar to that imaged in Fig. 5 (right).

It can be seen from Fig. 7 (top row left), that Sazhin's high-point was 5419 m AMSL in a quasi- linear updraft region just downwind of the NW-SE oriented east-ridge of Slide Mountain (altitude gain 4800 m, near Diamond Badge climb). The maximum predicted updraft at that location corresponded to ∼2.3 m/s and the maximum climb rate was 2.1 m/s passing through 4500 m AMSL (Table 1). The 4500 m altitude corresponds to approximately the 580 mb level where, from Fig. 7 (top row center), the winds were from 240 degrees-true at 47 knots. The GOES-E image, Fig. 7 (top row right) reveals a cloudless sky; the faint white regions are most likely snow on Slide Mountain and nearby ridges.

Shown in the bottom row of Fig. 7 is a forecast for the same region in light-wind conditions. It can be seen no linear updraft regions were predicted and no waves are visible in the GOES-E image; the snow-covered mountains are visible. The atmosphere was too dry and stable to support convection hence no convective clouds are visible.

It can be seen from Fig. 8 (left), that Sazhin's high-point was 5477 m AMSL in a linear updraft region just downwind of the NW-SE oriented east-ridge of Slide Mountain (altitude gain 4700 m, near Diamond Badge climb). The maximum predicted

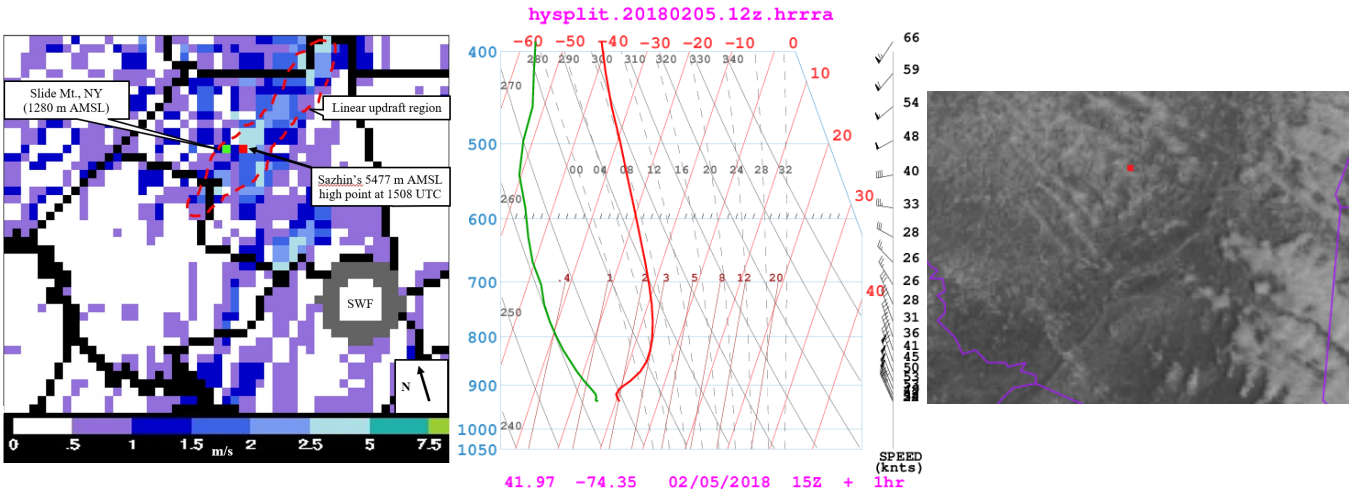

Fig. 8: Left, 20180205, HRRR model 5h forecast valid at 1500UTC (1000LT) for the maximum updraft speed (m/s) surface to 100 mb over the previous hour. Labeled is the high-point of Daniel Sazhin's flight (red pixel), the linear updraft region (dashed red line), the location of the mountain summit (green pixel) on the ridge that triggered the wave and Steward Field (SWF). Center, the atmospheric profile for the location, date and time of the high-point. Right, visible image at 1500UTC from GOES-E illustrating the approximate location of the high-point (red square).

updraft at that location corresponded to ∼3.8 m/s and the maximum climb rate was 3.0 m/s passing through 3250 m AMSL (Table 1). The 3250 m altitude corresponds to approximately the 680 mb level where, from Figure 8 (center), the winds were from 320 degrees-true at 26 knots. The GOES-E image, Fig. 8 (right), reveals cloud lines oriented in the direction of the boundary layer winds; there appear to be wave clouds above.

Discussion

The HRRR model characteristics are as follows. The model is run real-time, has 3-km resolution, is updated hourly and is cloud-resolving. The model is initialized with 3-km grids and with 3-km radar assimilation. The model covers the contiguous US. The model predicts hourly - for an 18-hour period - the major meteorological parameters. Hence, predictions made in the evening should be useful for next-morning flight decisions

Of the eight flights, five of the high-points were in linear updraft regions (Figs. 1, 2, 5, 6, 8) while three were in quasi-linear regions (Figs. 3, 4, 7). These coincidences prove the predicted updraft regions, indeed, were mountain waves.

On 9 February 2016, I e-mailed a HRRR model developer, Dr. John Brown of the NOAA- ESRL in Boulder CO, and asked how to interpret the 'maximum updraft/downdraft' predictions. Here is his helpful response: *"Care must be taken in interpreting these fields. For example, typical thermals of interest to glider pilots are fairly small, perhaps only a few hundred meters to a kilometer or two across. However, since the HRRR's computational points are 3km apart, such small-scale motions cannot be accurately predicted by the HRRR. The HRRR may try to represent such features, but they will be much larger in horizontal extent and in general contain weaker vertical motions than measured. In the case of mountain waves, the vertical velocity in vertically propagating mountain waves is fairly well represented, but trapped lee waves in general will not be well described because these waves are typically too small in horizontal wavelength to be well represented by a model with 3km grid spacing."*

Brown's statement is supported by the results in Table 1. The average of the measured updraft speeds was 2.3 m/s and the average of the predicted updraft speeds was 2.0 m/s. But there is no significant correlation between the measured and predicted speeds. When higher resolution predictions are available, the correlation is expected to become significant. Nevertheless, the HRRR model 'max updraft' predictions are consistent with the measurements. Hence, the prediction can be used to estimate whether a wave will be 'weak' or 'strong'.

The HRRR model 'max updraft' prediction presented here were calibrated as follows. Predictions on known wave days and expected non-wave days (predictions on fairly quiet - light wind - days) are compared in Figs. 1 (bottom) and 7 (bottom). It can be seen no linear or quasi- linear features appear in the light-wind predictions: mountain waves were not predicted. The scattered regions may be convective in origin.

Conclusions

The freely available HRRR NWP model predictions of 'max updraft' have been shown to identify regions and strengths of mountain waves. Hourly predictions are available for an 18-hour period. Hence, predictions of the location and strengths of mountain waves made in the evening should be useful for next-morning flight decisions.

Recommendations

This study is a first step. The next step is to increase the number of HRRR wave prediction- flight pairs and re-analyze the entire data-set using a Geographic Information System (GIS). This would result in the smallest possible navigation errors producing the best correlation between predicted and measured updrafts. A third step would be to compare HRRR updraft predictions and commercially available predictions (e.g., *Skysight*) with glider flight measurements. Sazhin, et al. [2] report Skysight demonstrates skill in predicting mountain waves. Finally, higher resolution NWP models will appear. At that time, the study should be repeated to determine the accuracy of the mountain wave forecasts and convective forecasts, as well.

Comparisons of NWP model results with glider flight data are expected to benefit the model developers.

Acknowledgements

The GOES-E images were from a number of sources: Figures 1 (right) and 2 (right) were courtesy of Timothy Chow; Figures 1 (bottom right), 4 (bottom right), 7 (bottom right) and 8 (right) were courtesy of Greg Thompson of the *UCAR*. All other images were downloaded from the *UCAR* site shortly after the flights (the archive contains hourly images for a day and for the past 5-days, as well).

References

[1] Lindsay, C., "Satellite wave observations used as an aid to wave soaring." *OSTIV Publications*, Vol. 8, 1965.

[2] Sazhin, D., Chidekel, P., and Bird, J., "Catskill Mountain wave project: Exploration, mapping, and forecasting of wave conditions in southern New York." *XXXIV OSTIV Congress Program and Proceedings*, 2018.

[3] Sazhin, D., "You gotta believe!" *Soaring*, Vol. 82, No. 5, 2018, pp. 16–19.

[4] Hindman, E., "Validating mountain-wave updraft speeds from the High-Resolution, Rapid-Refresh (HRRR) numerical weather prediction (NWP) model." *XXXIV OSTIV Congress Program and Proceedings*, 2018.

[5] Hindman, E. W., McAnelly, R., Cotton, W., Pattist, T., and Worthington, R., "An unusually high summertime wave fligh." *Technical Soaring*, Vol. 28, No. 4, 2004, pp. 7–23.